Indian Journal of Pure & Applied Physics
Vol. 44, July 2006, pp 501-508

Holographic optics based two-channel interferometer

Amit K Sharma, Sushil K Kaura, D P Chhachhia, C G Mahajan[#] & A K Aggarwal[*]

Coherent Optics Division, Central Scientific Instruments Organisation, Sector 30, Chandigarh 160 030

[#]Department of Physics, Panjab University, Chandigarh 160 014

Received 6 March 2006; accepted 12 May 2006

The paper describes a simple and cost effective method for making a two-channel interferometer based on holographic optics, which is suitable for performing optical test studies on two different phase objects simultaneously and independently. The optical arrangement in the proposed method involves a simple alignment procedure and inexpensive recording material is used in the formation of holographic optical elements. Recording schemes for the formation of holographic optical elements and the related techniques for the realization of the proposed interferometer along with the effect of misalignment of holographic optical elements and typical experimental results are presented.

Keywords: Optical interferometry, Two-channel interferometer, Holography, Optical testing instruments, Phase visualization

IPC Code: G03H

1 Introduction

Different types of optical interferometers are in use for the study of phase objects[1,2] as the interferograms provide accurate representation of the phase objects. The conventional optical interferometers generally use expensive and precise custom-made bulky optics and also involve rather tedious and time-consuming alignment procedures, which make them impractical in some applications. The use of holographic optical elements instead of the conventional optics can drastically reduce the bulkiness and high cost factors. Because of the several attractive features offered by holographic optical elements, such as light weight; compactness; ease of fabrication; containing multiple optical functions in a single element, their use provide the advantage in the construction of compact optical systems and their high functionality compared with conventional bulky optics. In recent years, there has been an increasing interest of using holographic optics based interferometers[3-6] for the study of phase objects in real time. These interferometers are generally suitable for performing optical test studies on a single phase object. A multi-channel optical interferometer[7,8] for the study of many phase objects simultaneously has been reported recently. This Young type interferometer, based on waveguide structures, is however suitable only for testing microstructure phase objects and not for the macro-structure objects. In this paper, we present a simple and cost effective method for making a compact and versatile two-channel interferometer based on holographic optics, which is suitable for performing optical test studies of two different macro size phase (transparent) objects simultaneously and independently. The proposed interferometer set-up has utility for comparative testing studies between two different phase objects in real time and may be useful in the studies of refractive index, wavefront measurements, thermal profiling, combustion, plasma diagnostics, atmospheric turbulence and flow visualization etc. The effect of misalignment of holographic optical elements on the interferograms has also been analyzed.

2 Principle of the Method

The method reported in this paper for making a two-channel interferometer is based on the formation of multiple holographic optical elements on two different recording plates in two recording steps. The first recording step involves the formation of two spatially separated holographic optical elements (H_{11} and H_{12}) on same recording plate H_1. The H_{11} and H_{12} are formed by using two different sets of collimated beams, O_1 with O_2 and O_3 with O_4 respectively, in conjunction with a common collimated beam R (Fig. 1). The plate H_1, containing these two permanently recorded HOEs, upon illumination with a single collimated beam R provides four in-built

Fax: + 91-172-2657267/2657082
[*]E-mail: aka1945@rediffmail.com

collimating beams O'_1, O'_2, O'_3 and O'_4 for subsequent recording. In the second recording step, the in-built collimated beam pairs O'_1 with O'_3 and O'_2 with O'_4 (generated from H_1) are used for the formation of two spatially separated holographic optical elements H_{21} and H_{22} on the second recording plate H_2 (Fig. 2). After processing, H_2 is repositioned at the same location at which it was recorded. These holographic plates H_1 and H_2 when placed in this configuration and illuminated with a single collimated beam R serves as a versatile two-channel interferometer (Fig. 3). Here H_1 upon illumination with R provides four illuminating beams, O'_1 and O'_2 from H_{11} and O'_3 and O'_4 from H_{12} for H_2. In this case, the so-generated beams O'_1 and O'_3 illuminate H_{21} and similarly O'_2 and O'_4 illuminate H_{22}. The illuminating beams O'_1 and O'_3

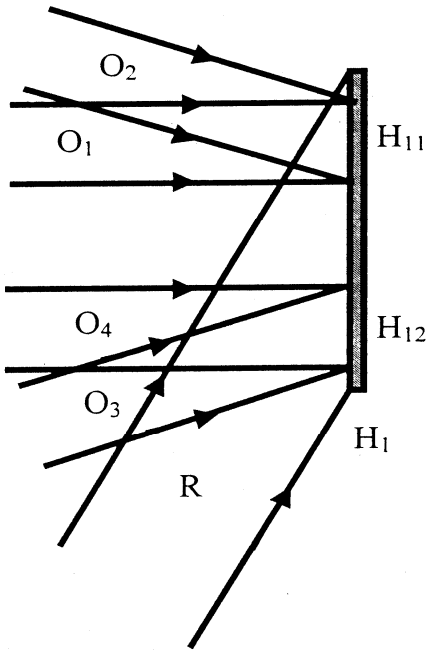

Fig. 1 — Schematic of forming holographic optical elements on H_1

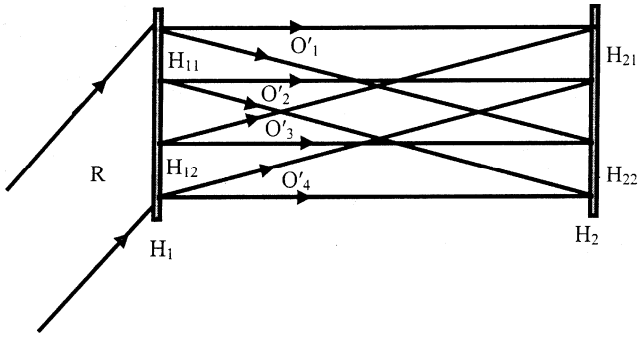

Fig. 2 — Schematic of forming holographic optical elements on H_2

on H_{21} further provide undiffracted-order beam O'_1 and diffracted-order beam O''_1 (due to O'_3) overlapping each other and also undiffracted-order beam O'_3 and diffracted-order beam O''_3 (due to beam O'_1) overlapping each other at two separate locations. Similarly at H_{22}, the illuminating beams O'_2 and O'_4 further provide undiffracted-order beam O'_2 and diffracted-order beam O''_2 (due to beam O'_4) which are overlapping each other and also undiffracted-order beam O'_4 and diffracted-order beam O''_4 (due to beam O'_2) overlapping each other at two separate locations. This results in the generation of four different interferograms at separate locations in the observation plane OP, which can be viewed on a screen or with a video camera.

Here O_1, O_2, O_3, O_4, O'_1, O'_2, O'_3, O'_4, O''_1, O''_2, O''_3, O''_4 and R are the complex amplitude distribution of the respective wavefronts. For simplicity, it is assumed that the holographic plates are developed in the linear region of the transmittance versus exposure curve. The amplitude transmittance of the processed H_1 is given[9] by:

$$t_1 \sim k\,[|O_1 + O_2 + R|^2 + |O_3 + O_4 + R|^2] \qquad \ldots(1)$$

where k is a parameter dependent on the recording material used, exposure and the processing conditions. For forming two spatially separated H_{21} and H_{22} on another recording plate H_2, the H_1 is illuminated only with a single collimated beam R (as was used in the first recording step). The complex amplitude of the transmitted field from H_1 is:

$$\begin{aligned} U_1 = R\,t_1 \approx k\,[R\,\{&|O_1|^2 + |O_2|^2 + |R|^2 + O_1^*\,O_2 + \\ &O_1^*\,R + O_2^*\,O_1 + R\,O_2^* + O_1\,R^* + O_2\,R^* + |O_3|^2 + \\ &|O_4|^2 + |R|^2 + O_4 O_3^* + R\,O_3^* + O_3\,O_4^* + R\,O_4^* + \\ &O_3\,R^* + O_4\,R^*\}] \end{aligned} \qquad \ldots(2)$$

It may be noted that the H_{11} and H_{12} are spatially separated and are recorded on a holographic recording plate H_1 in the form of holographic gratings. In the right hand side of Eq. 2 the first three terms [i.e., kR $(|O_1|^2 + |O_2|^2 + |R|^2)$] represent the undiffracted beam and the 4^{th} to 9^{th} terms represent the diffracted beams from H_{11}. In a similar manner, 10^{th} to 12^{th} terms (i.e. kR$(|O_3|^2 + |O_4|^2 + |R|^2)$) represent the undiffracted beam and 13^{th} to 18^{th} terms represent the diffracted beams from H_{12}. All these beams are spatially separated from each other. We can consider $|R|^2$ to be constant across the plate H_1, as a plane beam R is used

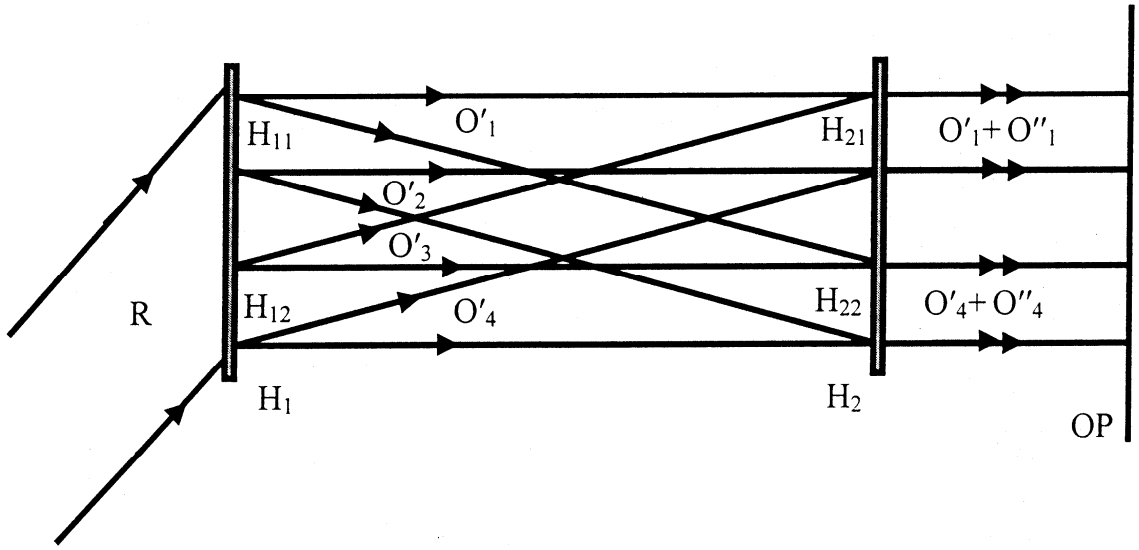

Fig. 3 — Schematic of a two-channel interferometer based on holographic optical elements

for the illumination of H_1. Thus, only the 8th, 9th, 17th and 18th terms on the right hand side of Eq. (2) are of interest to us as they represent the diffracted-order beams O'_1 and O'_2 generated from H_{11}; O'_3 and O'_4 generated from H_{12}, respectively. Here O'_1, O'_2, O'_3 and O'_4 are identical to the original respective beams O_1, O_2, O_3 and O_4 as they possess all the properties of these and can be considered to be as replica of the original beams and can be represented as:

$$kO_1|R|^2 + kO_2|R|^2 + kO_3|R|^2 + kO_4|R|^2 \approx O'_1 + O'_2 + O'_3 + O'_4 \quad \ldots(3)$$

The so-generated beams O'_1, O'_2, O'_3 and O'_4 are further used for forming two spatially separated HOEs on another recording plate H_2 in the second recording step (Fig. 2). After processing, H_2 is repositioned at the same location at which it was recorded. By using a similar analysis as followed for H_1, the amplitude transmittance of the processed H_2 is:

$$t_2 \approx k\,[|O'_1 + O'_3|^2 + |O'_2 + O'_4|^2] \quad \ldots(4)$$

In this configuration, when H_1 is illuminated with a collimated beam R, it provides four illuminating beams O'_1, O'_2, O'_3 and O'_4 for H_2 such that O'_1 and O'_3 illuminate H_{21} and O'_2 and O'_4 illuminate H_{22} respectively. The complex amplitude of the transmitted field from H_2 is given by:

$$U_2 = (O'_1 + O'_3)\,[k\,(|O'_1 + O'_3|^2)] + (O'_2 + O'_4)\,[k\,(|O'_2 + O'_4|^2)] \approx k\,[O'_1[|O'_1|^2 + |O'_3|^2] + O'_3|O'_1|^2 + O'_1{}^2\,O'_3{}^* + O'_3[|O'_1|^2 + |O'_3|^2] + O'_3{}^2\,O'_1{}^* + O'_1|O'_3|^2 + O'_2[|O'_2|^2 + |O'_4|^2] + O'_4|O'_2|^2 + O'_2{}^2 O'_4{}^* + O'_4[|O'_2|^2 + |O'_4|^2] + O'_4{}^2 O'_2{}^* + O'_2|O'_4|^2] \quad \ldots(5)$$

In right hand side of Eq. (5), the first term represents the undiffracted-order beam O'_1 and the sixth term represents the diffracted-order beam $O''_1 = O'_1 k|O'_3|^2 \approx O'_1$ (due to beam O'_3) and superimposes the above undiffracted-order beam O'_1. The second term represents the diffracted-order beam $O''_3 = O'_3\,k|O'_1|^2 \approx O'_3$ (due to beam O'_1) and the fourth term represents the undiffracted-order beam O'_3 and superimposes with the above diffracted-order beam O''_3. These spatially separated superimposed beam pairs generated from H_{21} thus provide two different interferograms at two separate locations in the observation plane OP. Similarly, the 7th term represents the undiffracted-order beam O'_2 and the 12th term represents the diffracted-order beam $O''_2 = O'_2\,k|O'_4|^2 \approx O'_2$ (due to beam O'_4) and superimposes the above undiffracted-order beam O'_2. The 8th term represents the diffracted-order beam $O''_4 = O'_4\,k|O'_2|^2 \approx O'_4$ (due to beam O'_2) and the tenth term represents the undiffracted beam O'_4 and superimposes the above diffracted beam O''_4. These spatially separated superimposed beam pairs generated from H_{22}, thus, also provide two different interferograms at separate locations in the observation plane OP. These four

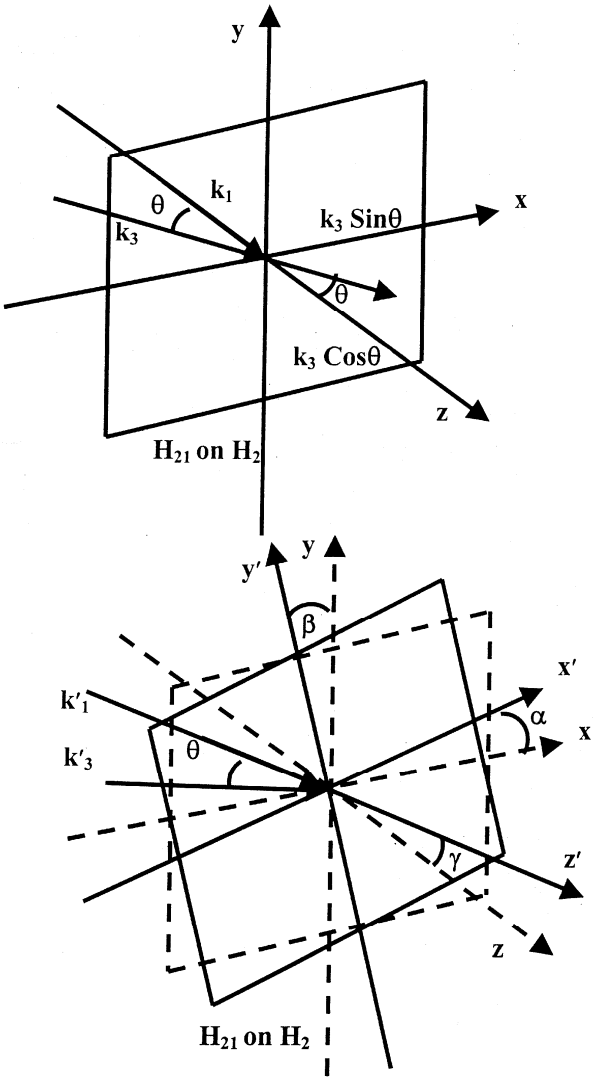

Fig. 4 — Schematic view of (a) initial orientation of H_{21} on plate H_2 and the related recording beams (b) reorientation of H_{21} on plate H_2 to eliminate fringes due to misalignment

interferograms generated in the observation plane OP are spatially separated from each other. By applying a simple alignment procedure in repositioning of H_2 results in infinite-fringe (i.e. zero fringe) interferograms (Fig. 4) in the observation plane. In this configuration, the portion of beams O'_1 and O'_4 generated between H_1 and H_2 can be used as two separate test arms for performing optical test studies on two different phase objects simultaneously. Typically, if a phase object $S = \exp[i\phi_1]$ is introduced in the first test arm O'_1 and a second phase object $P = \exp[i\phi_2]$ is introduced in the second test arm O'_4, then the complex amplitude of the transmitted field from H_2 is given by:

$$U_3 = (O'_1 S + O'_3)\, k\,[|O'_1 + O'_3|^2] + (O'_2 + O'_4 P)\, k\,[|O'_2 + O'_4|^2] \approx k\,[O'_1 S\,[|O'_1|^2 + |O'_3|^2] + O'_3 S|O'_1|^2 + O'^2_1 SO'^*_3 + O'_3\,[|O'_1|^2 + |O'_3|^2] + O'^2_3 O'^*_1 + O'_1|O'_3|^2 + O'_2\,[|O'_2|^2 + |O'_4|^2] + O'_4|O'_2|^2 + O'^*_4 O'^2_2 + O'_4 P[|O'_2|^2 + |O'_4|^2] + PO'^2_4 O'^*_2 + O'_2 P|O'_4|^2] \quad \ldots(6)$$

In the right hand side of Eq. (6), the 1st term represents the undiffracted-order beam O'_1 (containing information about phase object S) and the 6th term represents the diffracted beam O''_1 (generated due to O'_3 illuminating beam). Similarly, the 10th term represents the undiffracted beam O'_4 (containing information about phase object P) and the 8th term represents the diffracted beam O''_4 (generated due to O'_2 illuminating beam). Here, the beams O'_1 and O''_1 generated from H_{21} superimpose each other and similarly the beams O'_4, and O''_4 generated from H_{22} also superimpose each other and generate two different interferograms at separate locations in the observation plane. It may be noted that by following a similar procedure, two more spatially separated interferograms [due to O'_3 and O''_3 overlapping beams generated from H_{21} and also due to O'_2 and O''_2 overlapping beams generated from H_{22}] will be formed in the observation plane. For the sake of simplicity, we are considering only the upper two interferograms so as to explain the working phenomena. Thus, due to above, the complex amplitude distribution for the H_2 is:

$$U_4 \approx k\,[O'_1 S[|O'_1|^2 + |O'_3|^2 + O'_1|O'_3|^2] + k\,[O'_4 P[|O'_2|^2 + |O'_4|^2] + O'_4|O'_2|^2] \quad \ldots(7)$$

The intensity distribution, due to these interference patterns, in the observation plane is:

$$I_r = I_1 + I_2 \approx \{k^2 |O'_1 S|^2\,[|O'_1|^2 + |O'_3|^2]^2 + k^2 |O'_1|^2 |O'_3|^4 + k^2 |O'_1|^2 |O'_3|^2 [|O'_1|^2 + |O'_3|^2](S + S^*)\} + \{k^2 |O'_4 P|^2\,[|O'_2|^2 + |O'_4|^2]^2 + k^2 |O'_4|^2 |O'_2|^4 + k^2 |O'_4|^2 |O'_2|^2 [|O'_4|^2 + |O'_2|^2](P + P^*)\}$$

$$I_r \approx A + B\cos\phi_1 + C + D\cos\phi_2 \quad \ldots(8)$$

where A, B, C and D are constants. It is thus seen that the intensity distribution of the interference patterns,

recorded in the observation plane, depends only on the phase variation introduced by the phase objects S and P into the respective test beams O'_1 and O'_4 between H_1 and H_2. In order to realize the proposed interferometeric set-up, the processed HOEs are required to be repositioned at the same location at which these are formed. A slight misalignment in either H_1 or H_2 results in finite fringe interferograms in the observation plane. The effect of misalignment[10] in either of the HOEs, which results in finite fringe interferograms in the observation plane, is analyzed.

3 Alignment Sensitivity

For simplicity, the effects of misalignment in the plates H_1 and H_2 on one of the holographic optical elements say H_{21} on H_2 are considered. In this case, the interferogram gets formed due to superposition of undiffracted-order beam O'_1 and diffracted-order beam $O''_1 \approx O'_1$ (generated due to beam O'_3) can be represented as:

$$U \sim A^2 \psi O'_1$$

where, A is the amplitude of the beams O'_1 and O'_3; ψ is the distorting phase term[11] and is given by:

$$\psi \sim \exp i(\mathbf{k'_1}\,\mathbf{r'} - \mathbf{k_1}\,\mathbf{r}) + \exp i(\mathbf{k'_3}\,\mathbf{r'} - \mathbf{k_3}\,\mathbf{r}) \qquad \ldots(9)$$

where, $\mathbf{k_1}$, $\mathbf{k_3}$ and $\mathbf{r}$ represent the wavevectors of the illuminating beams and the position of the H_{21} in the recording condition, and $\mathbf{k'_1}$, $\mathbf{k'_3}$ and $\mathbf{r'}$ are the corresponding values for the reconstruction condition. The effect of misalignment in either H_1 or H_2 is separately analyzed.

(1) Misalignment in H_2

In this case (when H_2 is not properly repositioned after processing), the reconstructing beams are identical with the recording beams, i.e.,

$\mathbf{k'_1} = \mathbf{k_1}$ and $\mathbf{k'_3} = \mathbf{k_3}$, and the components [Fig. 4(a)] of the two vectors are:

$$\mathbf{k_1} \sim (0, 0, k_1)$$

$$\mathbf{k_3} \sim (k_3 \sin\theta, 0, k_3 \cos\theta)$$

Here the H_2 is assumed to be positioned perpendicular to the z-axis. This is not a general case, however, it is sufficiently close to the practical case. A more general treatment is possible but interpretation of results might be obscured by the complicated expressions. Since the illuminating source is coherent, thus $k_1 = k_3 = k$ and the misalignment vector associated with the H_2 plate position is: $\mathbf{r'} - \mathbf{r} = \mathbf{\Delta r}$

(a) Lateral position misalignment

In case, the plate co-ordinates are misaligned by a parallel translation i.e. $\Delta\mathbf{r} = (\Delta x, \Delta y, \Delta z)$ then ψ can be written as

$$\psi = \exp i\, k\Delta z + \exp i(k \sin\theta\, \Delta x + \cos\theta \Delta z)$$

Thus

$$|\psi|^2 = 4 \cos^2 k\, [\{\sin\theta\, \Delta x + (\cos\theta - 1)\, \Delta z\}/2]$$

Here repositioning is critical in the x and z directions as k_1 and k_3 differ in their x and z components. No fringe will occur (in the interferogram) in the observation plane when $\Delta x = (2n + 1)\, \pi/k \sin\theta$, and $\Delta z = (2n + 1)\pi/k\, (\cos\theta - 1)$; where n is an integer. To minimize the sensitivity with respect to x and z positioning, the components in these directions should be as small as possible.

(b) Rotation around x-axis

In case H_2 is rotated by an angle $\Delta\alpha$ along the x-axis then displacement vector

$$\Delta\mathbf{r} = (0, -z\Delta\alpha, + y\Delta\alpha)$$

Eq. (9) can now be written as:

$$\psi = \exp i\, k\, y\Delta\alpha\, (\cos\theta - 1) + 1$$

Thus, $|\psi|^2 = 4 \cos^2 [k\, y\Delta\alpha(\cos\theta - 1)/2]$

The sensitivity of ψ with respect to the rotation around the x-axis is thus of the first order of the rotation angle $\Delta\alpha$. Equally spaced fringes will appear parallel to the x-axis with spacing of $2\pi/k\Delta\alpha(\cos\theta - 1)$.

(c) Rotation around y-axis

When H_2 is rotated by an angle $\Delta\beta$ along the y-axis then displacement vector

$$\Delta\mathbf{r} = (z\Delta\beta, 0, - x\Delta\beta)$$

Eq. (9) can thus be written as:

$$\psi = \exp (ik \sin\theta\, z\Delta\beta) \exp [-i\, k\, x\Delta\beta(\cos\theta - 1)] + 1$$

Since the z-axis is perpendicular to the H_2 plane, thus only the projection of fringes onto the H_2 plane are observed.

Thus,

$$|\psi|^2 = 4 \cos^2 \{k\, [\sin\theta\, x\, (\Delta\beta)^2] - x\, \Delta\beta(\cos\theta - 1)\}/2$$

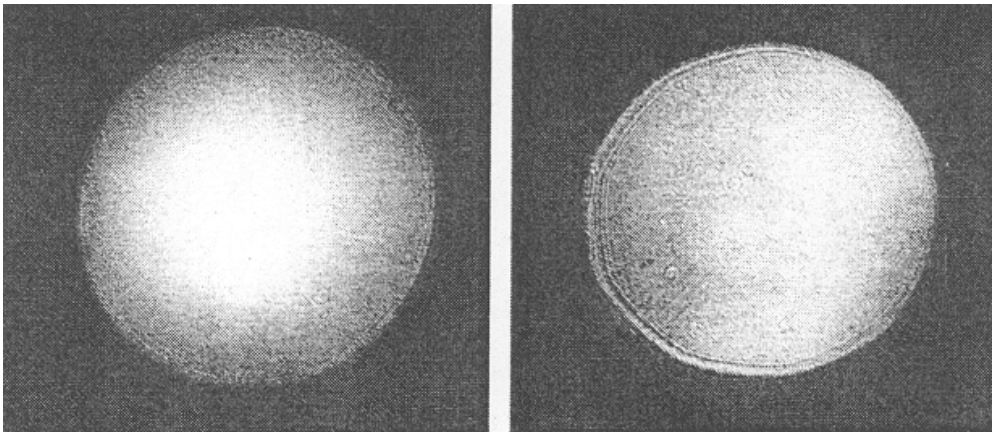

Fig. 5 — Typical infinite-fringe interferograms in the two channels

The sensitivity of ψ with respect to the rotation around the y-axis is thus of the second and first orders of the rotation angle $\Delta\beta$. Equally spaced fringes will appear parallel to the y-axis with a spacing of $2\pi/[k(\Delta\beta)\{\sin\theta\,\Delta\beta + (\cos\theta - 1)\}]$.

(d) Rotation around z-axis

When H_2 is rotated by an angle $\Delta\gamma$ along the z-axis then displacement vector:

$$\Delta\mathbf{r} = (y\Delta\gamma, -x\Delta\gamma, 0)$$

In this case, Eq. (9) can be written as:

$$\psi = \exp i\,(k \sin\theta\, y\Delta\gamma) + 1$$

Thus, $|\psi|^2 = 4\cos^2\{k(\sin\theta\, y\Delta\gamma/2\}$

The sensitivity of ψ with respect to the rotation around the z-axis is thus of the first order of the rotation angle $\Delta\gamma$. Equally spaced fringes will appear parallel to x-axis with spacing of $2\pi/(\sin\theta\,\Delta\gamma)$.

(2) Misalignment in H_1

In case, when there is any misalignment in H_1 and the H_2 is perfectly repositioned (i.e., $\mathbf{r} = \mathbf{r}'$), then the two illuminating beams on H_2 gets modified as:

$$\mathbf{k'}_1 - \mathbf{k}_1 = \delta\,\mathbf{k}_1 \text{ and } \mathbf{k'}_3 - \mathbf{k}_3 = \delta\,\mathbf{k}_3;$$

Eq. (9) can now be written as:

$$\psi = \exp i\,(\delta\,\mathbf{k}_1.\mathbf{r}) + \exp i\,(\delta\,\mathbf{k}_3.\mathbf{r})$$

Thus,

$$|\psi|^2 = 4\cos^2[(\delta\,\mathbf{k}_1 - \delta\,\mathbf{k}_3)\,\mathbf{r}/2] \qquad \ldots(10)$$

Eq. (10) depicts the presence of finite fringes (in the interferogram) in the observation plane, which may be in any direction depending upon the directions of $\mathbf{k'}_1$ and $\mathbf{k'}_3$. By using a simple geometrical analysis, it is observed that by providing a suitable rotation to the H_2 through angles α, β and γ with respect to the x, y, and z-axis [Fig. 4(b)]; the new coordinates x′, y′, z′ can be achieved in such a manner that the relative position of the H_2 with respect to the $\mathbf{k'}$ vectors is almost identical to the initial position with respect to the $\mathbf{k}$ vectors. This then facilitates in obtaining infinite fringe interferogram in the observation plane.

4 Experimental Details

In our experimental arrangement, a 35 mW He-Ne laser system was used in the first and second recording steps of the method for the formation of two different sets of spatially separated holographic optical elements on two different holographic plates H_1 and H_2. A large-size collimated beam (R) and four small-size collimated beams (O_1, O_2, O_3 and O_4) were generated by using a 100 mm-diameter and four 30 mm-diameter collimating lenses, respectively. The shear plate interferometric technique was applied to ensure the optical quality of the collimated beams, which were used for forming the holographic optical elements on H_1 and H_2. Standard Kodak D-19 developer and R-9 bleach bath solutions are used with Slavich PFG-01 plates (having spatial resolution power of more than 3000 mm^{-1}) to give high efficiency and low noise holographic optical elements (grating holograms) on H_1 and H_2. Holographic optical elements with almost uniform diffraction efficiency were generated using these holographic recording plates with exposure energies of the order of 100-120 $\mu J/cm^2$. In order to realize the proposed interferometer set-up, the processed H_2 plate is

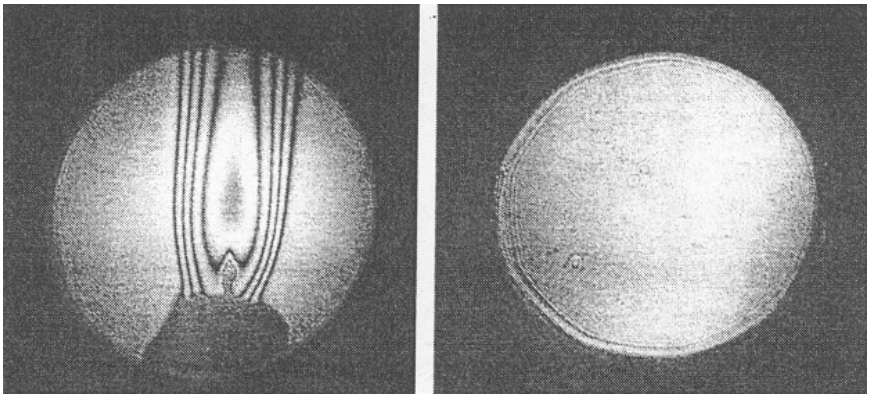

Fig. 6 — Typical interference pattern of heat flow due to a burning candle in one channel while second channel is without any object

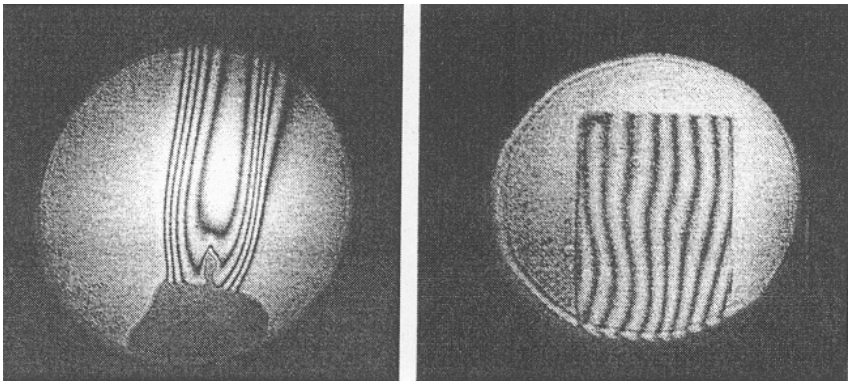

Fig. 7 — Typical interference pattern of heat flow due to a burning candle in one channel and a glass plate in the second channel

required to be repositioned at the same location at which it was formed. However, since in our recording scheme the interfering beams have permanently been frozen on a single element (H_1), the repositioning became much simpler. It was achieved by merely mounting the H_2 plate on a holder having the capabilities of providing tilt motion to the plate in horizontal and vertical directions. By using a simple alignment procedure, spatially separated infinite fringe interferograms are easily obtained in the observation plane [Fig. 5]. Optical test studies on two different phase objects were performed simultaneously and independently by inserting them in both the test arms between H_1 and H_2. In our studies, initially a burning candle was inserted in one of the test arm and no phase object was inserted in the other test arm. Typical interference patterns of heat flow caused by inserting a burning candle in one of the test arm and without inserting any phase object in the other test arm are shown in Fig. 6. It is seen from Fig. 6 that both the interferograms are independent of each other and any perturbation caused in any one of the test arms does not have any effect on the other test arm. Further studies were performed by inserting two different phase objects simultaneously and independently in both the test arms. Figure 7 shows typical interference patterns, in real time, obtained due to a burning candle in one of the test arm and a glass plate in the other test arm simultaneously and independently.

5 Conclusions

This paper presents a simple and cost effective method for making a compact and versatile two channel interferometer based on holographic optics, which is suitable for performing optical test studies of two different phase (transparent) phase objects simultaneously and independently. The advantage of this method lies in the fact that the proposed optical arrangement of the interferometer involves a very simple alignment procedure and portions of any one of the collimated beams O'_1 or O'_3 and O'_2 or O'_4

generated between H_1 and H_2 can be used as test arms for studying the phase objects. The effect of misalignment in H_1 or H_2 has also been studied and the infinite fringe interferograms are easily obtained by mounting the H_2 on a holder having the capabilities of providing tilt motion to the plate in horizontal and vertical directions and by following a simple alignment procedure. Wavefront distortions caused due to emulsion shrinkage/swelling and substrate etc get cancelled as the interfering beams pass through the same portions of the holographic optical elements on plate H_2. The interferometer is also suitable for performing comparison type studies of different phase objects in real time. It may be seen from Figs 6 and 7 that the proposed interferometric method, in infinite fringe mode set-up, gives high contrast interference patterns on insertion of different phase objects in any one of or both the test arms. Quantitative evaluation of the phase change may be performed by phase shifting interferometry, where it is possible to acquire a series of interferograms by giving a transverse displacement to the plate H_2 with a precision micrometer stage[12]. Further, the vital components of the interferometer could be produced in great numbers using hologram-copying methods[13].

Acknowledgement

The authors are grateful to the Director, CSIO, Chandigarh, for his constant encouragement, support and for permission to publish this work. They wish to thank Mr Raj Kumar for helpful discussions throughout the work and to CSIR and DST, New Delhi, for their financial support.

References

1 Malacara D (Ed), *Optical Shop Testing,* 2nd Ed (Wiley, New York) 1992, pp 51-206.

2 Robinson D W & Reid G T (Ed), *Interferogram analysis-Digital fringe pattern measurement techniques*, (Institute of Physics Publishing, Bristol and Philadelphia) 1993, pp. 141-193.

3 Zeilikovich I S & Platonov E M, *Optics & Laser Tech,* 17 (1985) 145.

4 Aggarwal A K, Kaura S K, Chhachhia D P & Sharma A K, *Optics & Laser Tech,* 36 (2004) 545.

5 Aggarwal A K, Kaura S K, Chhachhia D P & Sharma A K, "A robust interferometer based on holographic optics", *Experimental Techniques,* 29 (2005) 21-24.

6 Aggarwal A K, Kaura S K, Chhachhia D P & Sharma A K, *Current Sci,* 87 (2004) 228.

7 Ymeti A, Kanger S, Wijn R, Lambeck P V & Greve J, *Sensors and Actuators B,* 83 (2002) 1.

8 Ymeti A, Kanger S, Greve J, Lambeck P V, Wijn R & Heideman R G, *Appl Opt,* 42 (2003) 5649.

9 Hecht E & Zajac A, *Optics* (Addison-Wesley, Reading, Mass) 1974.

10 Dandliker R, Marom E & Mottier F M, *J Opt Soc Am*, 66 (1976) 23.

11 Politech J, Shamir J & Uri J B, *Optics & Laser Tech,* 3 (1971) 226.

12 Voirin G, Parriaux O & Vuilliomenit H, *Optical Engg,* (1995), 34 2687.

13 Caulfield H J (Ed), *Handbook of optical holography* (Academic Press, New York) 1979, pp 373-378.